PHYSICAL REVIEW B **95**, 155205 (2017)

Excitonic effects in the optical properties of hydrogenated anatase TiO_2

S. S. Ataei,[1,2,*] M. R. Mohammadizadeh,[1,†] and N. Seriani[2,‡]
[1]*Superconductivity Research Laboratory (SRL), Department of Physics, University of Tehran,*
North Kargar Ave., P.O. Box 14395-547, Tehran, Iran
[2]*The Abdus Salam International Centre for Theoretical Physics, Condensed Matter and Statistical Physics Section,*
Strada Costiera 11, 34151 Trieste, Italy

(Received 22 December 2016; published 19 April 2017)

Optical absorption spectra and excitonic properties of hydrogenated anatase titania have been calculated by *ab initio* calculations based on density functional theory, GW approximation, and the Bethe-Salpeter equation. Neutral hydrogen impurities lead to enhanced absorption in the infrared and visible regions, giving spectra compatible with experimental observations. Beside a broad signal in the infrared part, a sharp peak appears in the visible region that is due to excitonic effects. The wave functions of excitons in the infrared and in the visible are very localized, while those in the UV region are more delocalized than their counterparts in pure titania. It is argued that this could lead to a decreased electron-hole recombination of excitons in the UV, possibly leading to an increase in the photocatalytic activity of the material. On the contrary, positively charged hydrogen impurities barely modify the absorption spectrum, are probably difficult to be detected by optical absorption, and are unlikely to have a big effect on the photocatalytic properties of titania. These results contribute to understand the experimentally observed variability in the optical properties of hydrogenated titania and to obtain insight into their relation with the photocatalytic activity.

DOI: 10.1103/PhysRevB.95.155205

I. INTRODUCTION

Great research efforts are devoted to the tuning of the optical properties of titanium dioxide, a promising material for photocatalytic applications [1–5], with the aim to increase photoabsorption and the overall photocatalytic efficiency. In this context, black hydrogenated titania has attracted considerable attention recently [6–10], after the pioneering work by Chen *et al.* [6] in 2011 demonstrated a good efficiency in photocatalytic splitting of water. Meanwhile, hydrogenated titania specimens have been produced that display high photocatalytic activity but different optical properties. In the original work by Chen *et al.* [6], hydrogenated titania produced by a thermal treatment absorbed 24% of the visible portion of the solar spectrum and 1% of the infrared part. On the contrary, Wang *et al.* [8] employed a plasma treatment to hydrogenate titania to a likewise active form, resulting in a very strong absorption not only in the visible (39%) but also in the infrared (38%) region. Moreover, another open question regards nature and dynamics of excitons created by photon absorption, with respect to localization, recombination, and charge separation. In principle, it could be that the additional states and transitions from doping are strongly localized around the dopant atom, leading to increased recombination and thereby not being available for chemical reactions [5,11]. On the other side, hydrogen can act as an electron donor to titania; donated electrons in turn can form localized polarons or remain delocalized in the conduction band [12–15]. It is known that a localized surface plasmon resonance (LSPR) from a high concentration of electrons in the conduction band can induce absorption in the infrared region [8]. These properties are thus crucial for the functional behavior, because only long-lived electrons and holes can participate in the photocatalytic processes at the titania surface. It is therefore desirable to understand the origin of these differences in the optical properties and the consequences for the photocatalytic activity. Recent computer simulations based on density functional theory (DFT) have contributed to clarify the possible atomic structures of hydrogenated titania: Liu *et al.* [7] have shown that hydrogen may lead to disorder at a titania surface and in titania nanocrystals, with the breaking of Ti-O bonds and the formation of Ti-H and O-H bonds. Such a configuration leads to an extension of the valence band into the gap, a situation believed to correspond to the experiments of Ref. [6]. In bulk titania, the authors of the present paper showed that the electronic structure depends on the location of the hydrogen dopant, on its concentration, and on its charge state [16]. Neutral interstitial hydrogen (H_i) and low concentrations of neutral hydrogen in oxygen vacancies (H_O) lead to localized states in the band gap, while high concentrations of H_O ($0.125\ \frac{nH}{nTi}$) lead to the formation of delocalized states that effectively extend the conduction band into the gap. When the system becomes positively charged, the states in the gap disappear, and the band structure becomes very similar to that of pristine titania, with a slight increase of the band gap at high H_i^+ concentration.

While the electronic structure from DFT can deliver first hints at the optical properties of these systems, first-principles calculations of the photoabsorption are scant. Very recently, Mehta *et al.* [17] have calculated the photoabsorption spectrum of anatase in the presence of H_O, however at the level of the Fermi golden rule, i.e., making use of single-particle states and their energy differences from DFT only. At high concentration they obtained a substantial photoabsorption in the visible and in the infrared; the photoabsorption spectrum has quite a different shape from that measured in Ref. [6] and in Ref. [8], but it is in agreement with their own diffuse reflection spectra.

---

[*] sataei@ictp.it, samaneh.ataei@ut.ac.ir
[†] zadeh@ut.ac.ir
[‡] nseriani@ictp.it

In the present paper, we compute the optical properties of hydrogenated anatase by many-body perturbation theory in the GW approximation and the Bethe-Salpeter equation [18,19]. These methods were chosen to ensure that both the single-particle levels and the electron-hole interactions are properly described in the calculation [5,20,21]. We focus on the system at high hydrogen concentration (0.125 $\frac{\mathrm{nH}}{\mathrm{nT}i}$), because this was shown to display a wider variety of electronic structures [16]: localized gap states for $\mathrm{H_i}$, bandlike states below the edge of the conduction band for $\mathrm{H_O}$, and a band structure similar to pristine titania for the charged defects $\mathrm{H_i^+}$ and $\mathrm{H_O^+}$. In fact, here we show that the increasing photoabsorption at longer wavelengths measured in Ref. [8] appears in the presence of $\mathrm{H_i}$ and $\mathrm{H_O}$, even at the level of random-phase approximation, while the spectrum in the visible region displays sharp peaks only when the electron-hole interaction is explicitly considered. For these systems, the degree of localization of the exciton wave function varies, with very delocalized excitonic states in the ultraviolet (UV) part of the spectrum and localized excitonic states in the visible. This is in contrast with pure anatase, where the first bright exciton in the UV region has a 2D localized spatial behavior and might point to a lower electron-hole recombination in this region for hydrogenated titania [21,22]. This might be crucial for applications, because excitonlike trap states play an important role in limiting electron mobility in $\mathrm{TiO_2}$ [23–25]. Another result is that positively charged H defects are not easy to detect by optical measurements, because the absorption spectrum in their presence is very similar to that of pure titania. These results show that the photoabsorption spectrum measured in Ref. [8], with substantial absorption in the infrared and visible regions, is best explained by a high density of neutral hydrogen at oxygen vacancy sites. On the contrary, positively charged hydrogen impurities would not have appreciable effects on the photoabsorption of pure anatase. In the next section, the computational details are presented, then the calculation results are reported. Finally, a summary concludes the paper.

II. COMPUTATIONAL DETAILS

The ground state properties were investigated by density functional theory (DFT) using spin-polarized calculations and the Hubbard U correction (DFT+U) [26], as implemented in the QUANTUM-ESPRESSO package [27]. Calculation parameters were chosen to be the same as in our previous work [16]. The structures were fully relaxed with PBE+U. GW and Bethe-Salpeter equation calculations were performed with the YAMBO code [28]. Since for this code it is not possible to employ a DFT+U ground state calculation as input, we have performed self consistent field calculations with the PBE exchange-correlation functional [29] on the DFT+U structure. We have checked that PBE correctly reproduces the localized midgap states of DFT+U when employed on the PBE+U geometry. Single-shot $\mathrm{G_0W_0}$ calculations were performed with screening from a plasmon pole model [30]. The plasmon-pole (PP) approximation is known to qualitatively reproduce the main features of pristine $\mathrm{TiO_2}$, however with an overestimation of the electronic energy gap and the values of the renormalization factors (Z) [20]. Since in our work we are interested in distinguishing cases that are qualitatively very different, in this case the plasmon pole approximation is justified. Indeed, our calculated results for the Z values of pure anatase are in good agreement with the ones obtained by the full-frequency (FF) models (e.g., 0.73 for conduction band minimum) [20], and our calculated energy gap is 3.83 eV, 0.27 eV larger than the FF results, but in line with the results of other calculations with the plasmon pole approximation [21]. The total number of bands used for the calculations of both W and G were 200 for the defected systems and 120 for the perfect bulk. The energy cutoff for the correlation part of the self energy is 7 Ry while a total number of 6000 (for pure anatase) and 4500 (for hydrogenated titania) plane waves were used for the calculation of the exchange self-energy. The cutoff convergency was tested for both the electronic band structure with $\mathrm{G_0W_0}$ and the Bethe-Salpeter absorption spectra. A Monkhorst-Pack k-point mesh of (6×6×6) for bulk and (5×5×5) for the hydrogenated systems was used, while the convergency test for the absorption spectra with several k-points sampling [up to (7×7×7)] was done using the random-phase approximation (RPA). The optical spectra were calculated taking into account two-particle interactions, by solving the BSE on top of the GW calculations, as implemented in the YAMBO code [28]. We used 4 occupied and 22 empty bands for BSE calculations. The Drude term was modeled with a plasma frequency of $\hbar\omega_p = 3.94$ eV and a relaxation frequency of 0.7 eV [31]. This plasma frequency is determined by the calculated LSPR energy ($\hbar\omega_{sp} = 0.83$ eV) reported in Ref. [9] and the experimental dielectric constant of the perfect bulk (6) [32], using the method introduced in Ref. [33] to obtain the bulk plasma frequency.

III. RESULTS

We have investigated bulk anatase with a concentration of hydrogen of 0.125 $\frac{\mathrm{nH}}{\mathrm{nT}i}$, in the form of either neutral ($\mathrm{H_i}$) or positively charged ($\mathrm{H_i^+}$) defect at interstitial position, and in the form of neutral defect substituting oxygen ($\mathrm{H_O}$). This corresponds to a single hydrogen atom in a (2×1×1) supercell containing 8 $\mathrm{TiO_2}$ formula units, as in our previous work [16].

A. Quasiparticle energy levels

In Fig. 1, the electronic band structures of the defected systems using the $\mathrm{G_0W_0}$ approximation are shown. The three band structures are considerably different: for $\mathrm{H_i^+}$ it is very similar to pristine anatase, apart from an increase of the band gap by 0.3 eV; for $\mathrm{H_i}$ there is an occupied defect state slightly below the conduction band minimum (CBM), while for $\mathrm{H_O}$ bandlike states develop from the presence of hydrogen. This is qualitatively similar to what was obtained by DFT+U [16], with some remarkable differences. For $\mathrm{H_i}$, GW yields an occupied defect level at about 0.2 eV below the CBM, which is shallower than our PBE+U results (0.9 eV below the CBM) [16]. This state would then be identified by GW as a shallow donor state. Experimental data on hydrogenated anatase give intermediate values: Lavrov [34] found infrared (IR) absorption lines at 3412 and 3417 $\mathrm{cm^{-1}}$, which correspond to 0.42 eV, however at a lower concentration of hydrogen. Miyagi *et al.* [35] reported deep-level transient spectroscopy

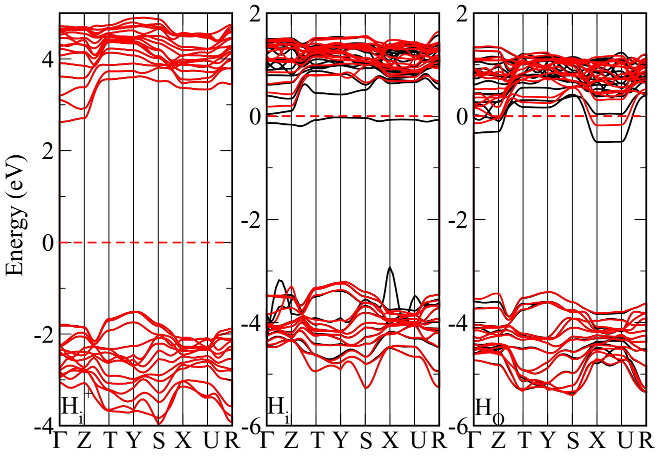

FIG. 1. Band structure of H_i^+, H_i, and H_O-doped titania calculated using the GW method, from left to right, respectively. The zero of energy is set to the Fermi level. The black lines correspond to spin up and the red ones correspond to spin down electronic structure.

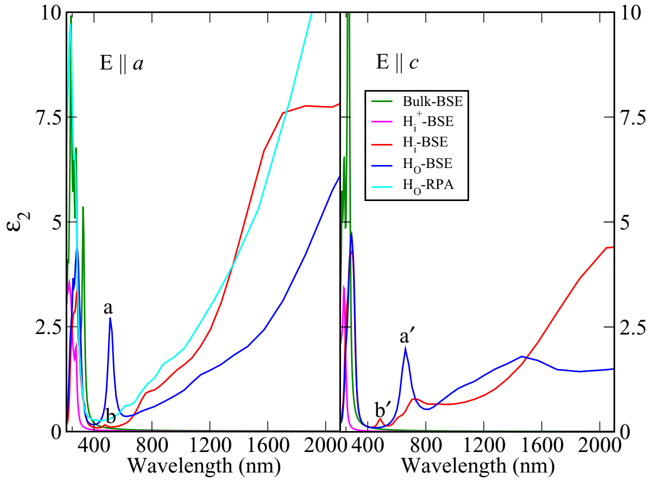

FIG. 2. The calculated absorption spectra of perfect and hydrogenated titania as a function of wavelength. The letters indicate peaks referred to in the text: (a) excitonic peak in the visible range appearing at the level of Bethe-Salpeter equation for the H_O defect for in-plane polarization of the incoming radiation; (b) excitonic peak in the visible range appearing at the level of Bethe-Salpeter equation for the H_i defect for in-plane polarization of the incoming radiation; (a′) excitonic peak in the visible range appearing at the level of Bethe-Salpeter equation for the H_O defect for out-of-plane polarization of the incoming radiation; (b′) excitonic peak in the visible range appearing at the level of Bethe-Salpeter equation for the H_i defect for out-of-plane polarization of the incoming radiation.

(DLTS) data with a peak at 0.5 eV for hydrogenated titania. The defect level disappears for H_i^+ with an electronic band gap which is a bit larger (about 0.3 eV) than the one for the perfect bulk. On the contrary, for H_O there is a band gap narrowing of about 1 eV with respect to the perfect bulk, which is completely in agreement with our PBE+*U* results [16]. The renormalization factors, which are an indicator of the single-particle character of the quasiparticles [18], are about 0.5 for the occupied and empty states (Γ *k* point) around the Fermi levels of H_O and H_i. These values are smaller than the calculated *Z* factors for the pristine titania and for the system with H_i^+ (about 0.7). This might be because Ti 3*d* states are involved in the midgap states, and 3*d* states in transition metals have typical values of the renormalization factors of about 0.5 [36].

TABLE I. The calculated optical transitions including excitonic effects, in which occ means the occupied bands below the Fermi level, unocc means the empty states above the Fermi level, and mid means impurity states crossing the Fermi level.

System	Energy, eV (nm)	*K* points	Bands
Bulk (*xy*)	3.8 (326.27)	Γ-*Z*	1st, 2nd (occ) → 1st, 2nd (unocc)
Bulk (*z*)	4.49 (276.13)	Γ-*Z*, Γ-*X*	1st, 2nd (occ) → 2nd, 3rd (unocc)
	4.63 (267.78)	Γ-*X*	1st, 2nd (occ) → 1st, 2nd (unocc)
H_i^+-doped (*xy*)	4.24 (292.42)	Γ-*Z*	2nd (occ) → 1st (unocc, ↑)
	4.48 (276.75)	Γ-*Z*	2nd, 3rd (occ) → 1st (unocc, ↑)
H_i^+-doped (*z*)	4.87 (254.59)	Γ-*X*	2nd (occ) → 1st (unocc, ↑)
	5.27 (235.26)	Γ-*X*	2nd (occ) → 3rd (unocc, ↑)
H_i-doped (*xy*)	0.5 (2.48e+3)	Γ-*X*	1st (mid) → 2nd (mid, ↑)
	2.61 (475.04)	...	...
	3.69 (336.00)	Γ-*Z*	1st, 2nd (occ) → 1st (unocc, ↑ , ↓)
H_i-doped (*z*)	0.5 (2.48e+3)	Γ	2nd (mid) → 1st (unocc, ↑)
	1.76 (704.46)	Γ-*Z*, Γ-*Y*	1st (mid) → 18th, 20th (unocc, ↓ , ↑)
	2.5 (495.94)	...	...
	3.99 (310.74)	Γ-*X*, Γ-*Y*	1st, 2nd (occ) → 1st (unocc, ↓)
H_O-doped (*xy*)	0.02 (6.20e+4)	Γ-*Z*	3rd (mid) → 1st (unocc, ↑)
	2.4 (516.6)	...	...
	4.03 (307.65)	Γ-*R*, Γ-*X*, Γ	1st, 2nd (occ) → 1st (mid,unocc, ↑)
H_O-doped (*z*)	0.07 (1.77e+4)	Γ-*X*	2nd (mid) → 3rd (mid, ↑)
	1.88 (659.49)	Γ-*Z*	1st (mid) → 19th (unocc, ↓)
	3.99 (310.74)	Γ-*R*, Γ-*Z*	2nd, 3rd (occ) → 1st, 3th (mid,unocc, ↓)

B. Optical properties

The absorption spectra of perfect anatase and of the hydrogenated systems are shown in Fig. 2, for the two main polarization directions in the tetragonal cell, as calculated by solving the Bethe-Salpeter equation. In order to better understand excitonic effects, for one case, namely for the in-plane (E parallel to a) polarization of H_O, the absorption was also calculated at the level of RPA, which does not describe the electron-hole interaction.

The spectrum of pure titania is in agreement with experiments and with previous calculations [20,21,37]; for the in-plane polarization, it displays the first direct optical transition at 3.8 eV, which is the most intense excitonic state with transition from the two highest states of the valence band to the two lowest levels of the conduction band with the k points along the Γ-Z direction. There are then two optical transitions at 4.49 eV and 4.63 eV, which have a counterpart in the spectrum for out-of-plane polarization in the intense peak at 4.67 eV.

The spectrum for the H_i^+-doped system confirms that protons lead to a slightly increased band gap, but to no other noticeable effect. In particular, it does not bring any absorption in the visible and infrared regions. It seems that H_i^+ does not improve the absorption properties of titania in any way. Moreover, these calculations suggest that it would be difficult to detect the presence of interstitial protons by optical measurements. This also implies that the measured absorption spectra can only be explained by the presence of other kinds of hydrogen defects. The calculated exciton binding energy (with in-plane polarization) of this system is 0.19 eV while the one for the bulk is 0.1 eV. Indeed, the neutral H_O and H_i defected systems display absorption also in the visible and infrared regions. The two regions also display important differences. Absorption in the infrared region consists in a broad signal, present in both polarizations, increasing at longer wavelengths. This broad signal is also present at RPA level, showing that, for that part of the spectrum, excitonic effects are not very important. On the contrary, in the visible region a sharp peak appears only in the BSE results [e.g., at 515 nm for H_O with in-plane polarization, peak (a) in Fig. 2], unmistakenly testifying excitonic effects. Our spectra are most similar to those measured by Wang *et al.* [8]. Strong absorption in a broad infrared region, with absorption increasing at longer wavelengths, is in agreement with their measurements. On the contrary, the sharp peaks observed in the visible region, and due to excitonic effects, do not appear in the experimental spectra [6,8]. There might be, however, good reasons why our sharp peaks might not appear in the experimental results. First, their position depends on the polarization, and the experiments are performed on a nanocrystalline sample, thereby effectively yielding a spectrum averaged over polarizations, thereby smearing out the sharp peaks. Second, our results are at zero temperature, whereas the electron-phonon interaction in titania is likely to play an important role at finite temperature [20,38]. This discrepancy is not a unique feature of our work: Also in (Si,Ni) co-doped titania the calculations at single-particle level show a peak in the visible region which does not appear in the experiments [4]. Our calculation also slightly overestimates the imaginary part of the dielectric function at very low energies, a fact which might be related to the overestimation of intraband transitions described by the Drude model. This has also been reported for other systems (e.g., MnGaAs) [39]. The calculated exciton binding energies of the neutral H_O and H_i defected systems are 0.37 eV and 0.15 eV, respectively.

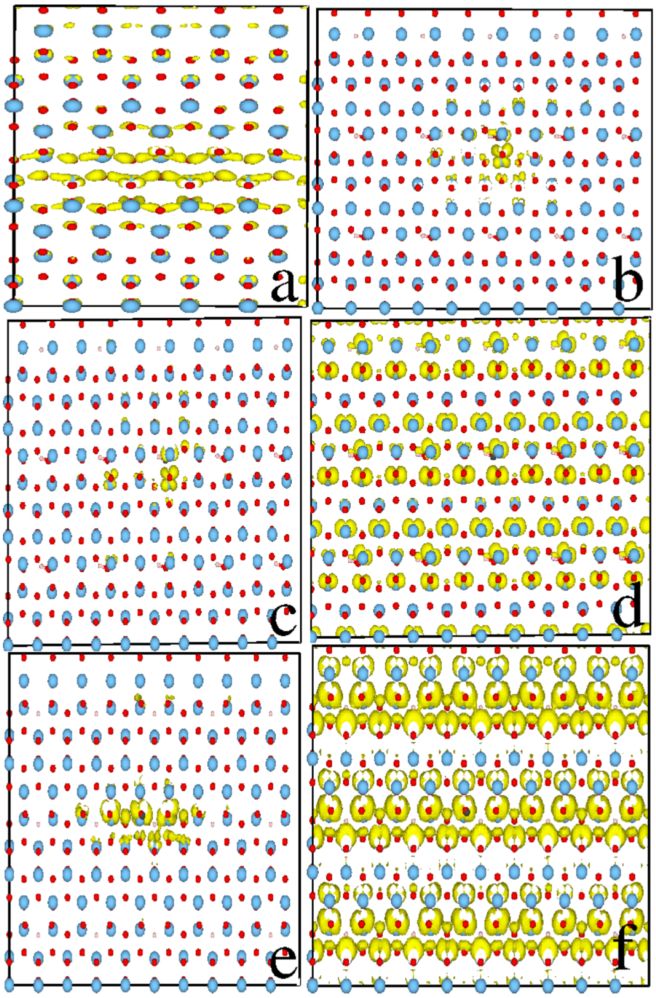

FIG. 3. Spatial distribution of excitonic states of (a) perfect bulk at 3.8 eV, (b) H_i^+-doped system at 4.24 eV, (c) H_i-doped system at 2.6 eV, (d) H_i-doped system at 3.69 eV, (e) H_O-doped system at 2.4 eV, and (f) H_O-doped system at 4.03 eV, with in-plane polarization.

To better characterize energy levels, k points, and wave functions involved in the optical transitions, the Bethe-Salpeter Hamiltonian has been exactly diagonalized. The calculated excitonic transition states are reported in Table I. For H_i^+, the bright excitons in the UV correspond to transitions from the two highest occupied bands (mostly $2p$ orbitals of the oxygen atoms) to the two lowest empty states ($3d$ orbitals of Ti atoms). This confirms that the effects of H_i^+ are negligible and that these transitions are standard for oxides like this. On the contrary, the neutral defected systems display a richer phenomenology: The first bright excitons in the infrared region are due to collective excitations of shallow donor states (Ti $3d$ states). These states are filled by electron donation from hydrogen. For example, for the H_O defect and the out-of-plane polarization [peak (a′) in Fig. 2, corresponding to the transition at 1.88 eV in Table I], a single impurity state and a single empty state make up over two thirds of the excitonic wave function; in turn, Ti-3*d* orbitals compose more than three quarters of the impurity state and roughly two thirds of the empty state from the conduction band. In addition, the bright excitons at 2.6 eV, 2.5 eV, and 2.4 eV, which correspond to the enhanced visible-light absorption peaks, are due to transitions from shallow donor states (Ti 3*d* states) to the higher-lying empty bands (Ti 3*d* states). At higher energies, in the UV region, the transitions from 2*p* states of the oxygen atoms to the 3*d* levels of Ti atoms appear again, like in the other cases. However, in the UV energy range there are differences, namely in the nature of the excitons. This can be understood from the spatial distribution of the exciton wave functions related to the main peaks of the absorption spectra (Fig. 3). Indeed, the wave function of the first excitonic state of perfect anatase is spatially localized in the XY plane (Fig. 3(a) and Ref. [21]). For H_i^+, the first exciton is more localized than that of pure anatase [Fig. 3(b)]; this should increase the rate of electron-hole recombination [22]. The behavior of H_O and H_i is more complex, with the excitons in the infrared and visible ranges being very localized [peaks (a), (b), (a′), and (b′) in Fig. 2], while those in the UV are more delocalized than the corresponding transitions in pure anatase. This result suggests that a high concentration of neutral hydrogen defects in anatase TiO_2 should lead to lower electron-hole recombination in the UV part of the spectrum, which might be useful for, e.g., photocatalytic applications that need long-lived electrons and holes to react with the molecules on the surface.

IV. SUMMARY

We have investigated the optical properties of hydrogenated titania by means of *ab-initio* methods based on density functional theory, the GW approximation, and the Bethe-Salpeter equation (BSE). A high concentration of hydrogen defects (0.125 $\frac{\mathrm{nH}}{\mathrm{nT}i}$) has been considered to be present in bulk anatase, as neutral (H_i) or positively charged (H_i^+) defect at interstitial position, and in the form of neutral defect substituting oxygen (H_O). The positively charged defect leads only to minor changes in the optical absorption spectrum of pure titania, consisting in a small increase of the band gap, by about 0.3 eV, and in more localized exciton states. This seems to indicate that it should be very difficult to detect the presence of protons in anatase in photoabsorption experiments, and that their effect, if any, would rather be to decrease the photocatalytic efficiency by increasing recombination. On the other side, the neutral defects H_i and H_O yield an increased absorption in the visible and the infrared ranges, with spectra compatible with those measured in Ref. [8]. Hydrogen donates electrons to shallow Ti 3*d* states, and excitations from these states into Ti-3*d*-dominated conduction band states are mainly responsible for the increased photoabsorption. In the visible range, BSE results give a sharp peak due to excitonic effects; this peak is not present in the experimental spectra, maybe because of overlap of different polarizations or due to the electron-phonon interactions. The wave function related to this excitonic peak is composed mainly by Ti-3*d* states. While wave functions of excitons in the infrared and visible range are very localized, exciton wave functions in the UV region are more delocalized than in pure anatase, a fact which should contribute to decrease electron-hole recombination and possibly increase availability of electrons and holes for photocatalytic reactions.

ACKNOWLEDGMENTS

M.R.M. and S.S.A. acknowledge partial financial support by the research council of the University of Tehran,"Center of Excellence on the Structure and Physical Properties of Matter" of the University of Tehran and the ICTP-IAEA Sandwich Training Educational Programme (STEP).

[1] V. Subramanian, E. E. Wolf, and P. V. Kamat, J. Am. Chem. Soc. **126**, 4943 (2004).
[2] J. Yu, G. Dai, and B. Huang, J. Phys. Chem. C **113**, 16394 (2009).
[3] J. Yu, H. Tao, and B. Cheng, ChemPhysChem **11**, 1617 (2010).
[4] Y. Lin, Z. Jiang, C. Zhu, X. Hu, X. Zhang, H. Zhu, Haiyan, and J. Fan, Appl. Phys. Lett. **101**, 062106 (2012).
[5] Z. Yong, P. E. Trevisanutto, L. Chiodo, I. Santoso, A. R. Barman, T. C. Asmara, S. Dhar, A. Kotlov, A. Terentjevs, F. Della Sala, V. Olevano, M. Rubhausen, T. Venkatesan, and A. Rusydi, Phys. Rev. B **93**, 205118 (2016).
[6] X. B. Chen, L. Liu, P. Y. Yu, and S. S. Mao, Science **331**, 746 (2011).
[7] L. Liu, P. Y. Yu, X. Chen, S. S. Mao, and D. Z. Shen, Phys. Rev. Lett. **111**, 065505 (2013).
[8] Z. Wang, C. Yang, T. Lin, H. Yin, P. Chen, D. Wan, F. Xu, F. Huang, J. Lin, X. Xie, and M. Jiang, Adv. Funct. Mater. **23**, 5444 (2013).
[9] X. Ma, Y. Dai, L. Yu, and B. Huang, Sci. Rep. **4**, 3986 (2014).
[10] C. Fan, C. Chen, J. Wang, X. Fu, Z. Ren, G. Qian, and Z. Wang, Sci. Rep. **5**, 11712 (2015).
[11] E. W. McFarland and J. Tang, Nature (London) **421**, 616 (2003).
[12] C. Di Valentin and A. Selloni, J. Phys. Chem. Lett. **2**, 2223 (2011).
[13] A. Janotti, C. Franchini, J. B. Varley, G. Kresse, and C. G. Van de Walle, Phys. Status Solidi RRL **7**, 199 (2013).
[14] M. Setvin, C. Franchini, X.-F. Hao, M. Schmid, A. Janotti, M. Kaltak, C. G. Van de Walle, G. Kresse, and U. Diebold, Phys. Rev. Lett. **113**, 086402 (2014).
[15] S. Selcuk and A. Selloni, Nat. Mater. **15**, 1107 (2016).
[16] S. S. Ataei, M. R. Mohammadizadeh, and N. Seriani, J. Phys. Chem. C **120**, 8421 (2016).
[17] M. Mehta, N. Kodan, S. Kumar, A. Kaushal, L. Mayrhofer, M. Walter, M. Moseler, A. Dey, S. Krishnamurthy, S. Basu, and A. P. Singh, J. Mater. Chem. A **4**, 2670 (2016).
[18] G. Onida, L. Reining, and A. Rubio, Rev. Mod. Phys. **74**, 601 (2002).

[19] M. Rohlfing and S. G. Louie, Phys. Rev. B **62**, 4927 (2000).

[20] W. Kang and M. S. Hybertsen, Phys. Rev. B **82**, 085203 (2010).

[21] L. Chiodo, J. M. García-Lastra, A. Iacomino, S. Ossicini, J. Zhao, H. Petek, and A. Rubio, Phys. Rev. B **82**, 045207 (2010).

[22] A. Molina-Sánchez, D. Sangalli, K. Hummer, A. Marini, and L. Wirtz, Phys. Rev. B **88**, 045412 (2013).

[23] C. Richter and C. A. Schmuttenmaer, Nat. Nanotechnol. **5**, 769 (2010).

[24] N. Hosaka, T. Sekiya, and S. Kurita, J. Lumin. **72-74**, 874 (1997).

[25] L. Cavigli, F. Bogani, A. Vinattieri, L. Cortese, M. Colocci, V. Faso, and G. Baldi, Solid State Sci. **12**, 1877 (2010).

[26] V. I. Anisimov, J. Zaanen, and O. K. Andersen, Phys. Rev. B **44**, 943 (1991).

[27] P. Giannozzi, S. Baroni, N. Bonini, M. Calandra, R. Car, C. Cavazzoni, D. Ceresoli, G. L. Chiarotti, M. Cococcioni, I. Dabo, A. D. Corso, S. de Gironcoli, S. Fabris, G. Fratesi, R. Gebauer, U. Gerstmann, C. Gougoussis, A. Kokalj, M. Lazzeri, L. Martin-Samos, N. Marzari, F. Mauri, R. Mazzarello, S. Paolini, A. Pasquarello, L. Paulatto, C. Sbraccia, S. Scandolo, G. Sclauzero, A. P. Seitsonen, A. Smogunov, P. Umari, and R. M. Wentzcovitch, J. Phys.: Condens. Matter **21**, 395502 (2009).

[28] A. Marini, C. Hogan, M. Grüning, and D. Varsano, Comput. Phys. Commun. **180**, 1392 (2009).

[29] J. P. Perdew, K. Burke, and M. Ernzerhof, Phys. Rev. Lett. **77**, 3865 (1996).

[30] H. N. Rojas, R. W. Godby, and R. J. Needs, Phys. Rev. Lett. **74**, 1827 (1995).

[31] A. Stroppa, S. Picozzi, A. Continenza, M. Y. Kim, and A. J. Freeman, Phys. Rev. B **77**, 035208 (2008).

[32] R. J. Gonzalez, R. Zallen, and H. Berger, Phys. Rev. B **55**, 7014 (1997).

[33] J. M. Luther, P. K. Jain, T. Ewers, and A. P. Alivisatos, Nat. Mater. **10**, 361 (2011).

[34] E. V. Lavrov, Phys. Rev. B **93**, 045204 (2016).

[35] T. Miyagi, M. Kamei, T. Mitsuhashi, and A. Yamazaki, Appl. Phys. Lett. **88**, 132101 (2006).

[36] V. I. Anisimov, in *Strong Coulomb Correlations in Electronic Structure Calculations* (CRC Press, Boca Raton, Florida, 2000), p. 41.

[37] N. Hosaka, T. Sekiya, C. Satoko, and S. Kurita, J. Phys. Soc. Jpn. **66**, 877 (1997).

[38] C. Di Valentin, G. Pacchioni, and A. Selloni, J. Phys. Chem. C **113**, 20543 (2009).

[39] P. Rosa, D. Sangalli, G. Onida, and A. Debernardi, Phys. Rev. B **91**, 075207 (2015).